Vector Hydrophone Passive Time Reversal for Underwater Acoustic Communications

Fabricio A. Bozzi and Sergio M. Jesus

Laboratory for Robotic Systems in Engineering and Science (LARSyS)

University of Algarve

8005-139 Faro, Portugal

fabozzi@ualg.pt, sjesus@ualg.pt

Abstract—The use of vector hydrophones as a receiver for underwater communications has been the subject of research since such device is a compact option to pressure-only arrays. A vector hydrophone, usually called acoustic vector sensor, is a device that measures pressure and particle velocity components. This paper investigates a method to combine those channels based on passive time-reversal (PTR). Simulation and experimental data are used to quantify communication performance, comparing vector hydrophones to pressure-only arrays. The analyzed acoustic scenario consists of a shallow-water area (about 100 m), where a vector hydrophone array receives communication signals from a bottom moored source. Simulations help in the understanding of diversity by analyzing spectral characteristics of vector hydrophone channels and the PTR q-function. While in simulation, the benefits of PTR using particle velocity channels are perceptible seen by exploring diversity, communication performance with experimental data is degraded due to time-varying. Finally, the achieved performance using a single or a small array of vector hydrophones enforces its benefits for communication enhancement.

Index Terms—vector hydrophone, passive time reversal, underwater acoustic communications

I. INTRODUCTION

The use of vertical hydrophone arrays is a common approach to improve underwater acoustic communication (UWAC) performance. This improvement is due to a spatial gain dependent on the adopted signal processing and the underwater channel. The best processor is able to enhance the signal-to-noise ratio (SNR) and eliminate, or at least reduce intersymbol interference (ISI). In this regard, passive time-reversal (PTR) is a method that may provide both effects, usually by exploring spatial diversity [1].

Spatial diversity may be interpreted in different ways depending on the application. Here, spatial diversity is obtained when a signal travels throughout the channel, and sensors receive it with diverse characteristics. These received signals are different from each other due to different paths (and iteration with bottom and surface) and the receiver positions. Furthermore, transmission loss, interference, and fading differ among receivers. Thus, increasing the number of receivers (and the spacing) tends to grow the probability of recovering the transmitted signal. Moreover, combining those diverse signals may be interesting rather than selecting the best one. In this sense, spatial diversity combining techniques are commonly used in UWAC, in which some authors include the PTR [2]–[4].

Passive time-reversal using hydrophone arrays has proved to enhance UWAC performance, especially when long arrays are used along the water column. However, deployment of such arrays may be a challenging task or simply unsuitable, e.g., for size-restricted applications such as autonomous underwater vehicles. When PTR is used with hydrophone arrays, called hereafter pressure-only arrays, PTR focusing resolution is related to the array length and the sensor spacing (also viewed as dependent on signal coherence length). A full study of the relation between the array configuration and PTR performance can be found in [3]. Thus, size reduction leads to unavoidable performance degradation. In this sense, vector hydrophones (usually called acoustic vector sensors - VS[1]) may improve performance compared to pressure-only arrays [5].

A vector hydrophone is a device that measures pressure and particle velocity components, where directional information is provided by particle velocity. Vector hydrophones usually measure two or three orthogonal particle velocity components, which combined with the pressure channel can provide sound wave direction. The best way to combine those channels is still a research subject and depends on the application. While sonar applications commonly use beamforming, for communications authors also try to explore a different type of diversity among VS channels [5]. In theory, the diversity among VS channels is explained by channel correlation. However, this VS diversity is not clearly visualized and quantified using experimental data.

Motivated by the applicability of vector sensors for communications, this study investigates the PTR method using vector hydrophones. The present work quantifies communication performance using simulated and recorded data from a field experiment (MakaiEx) [5]. This performance is analyzed and compared using a single VS, four vector sensors, and a pressure-only array of four elements (pressure components of the vector sensor array - VSA). The objective is to show how and when vector hydrophones can provide diversity and what is the effect of this diversity on performance.

---

[1]Readers may observe that vector hydrophones and vector sensors (VS) are interchangeably used in this paper.

II. Theoretical Framework

This section presents the adopted VS data model, useful measures to quantify VS channels, and the VS PTR method.

A. Vector hydrophone data model

A vector hydrophone measures pressure using an omni-directional hydrophone and two or three particle velocity components. Among different technologies, commonly particle velocity is measured using inertial sensors or a pair of hydrophones [6]. While the former is said to provide a "true" particle velocity by sensing the movement (or velocity or acceleration), the latter provides a particle velocity estimation by subtracting the hydrophone outputs. Although each VS technology presents pros and cons, the principle of both is based on the Euler's equation, where $\nabla p = -j\omega\rho_0\mathbf{v}$, being ∇ the gradient operator, p the pressure, ρ_0 the medium static density, ω the angular frequency, and $\mathbf{v}$ the particle velocity vector. Thus, we can take the particle velocity directly from an inertial sensor or take the pressure gradient using a pair of hydrophones.

The input-output data model is given by:

$$r_n = h_n \otimes s + w_n, \tag{1}$$

where r is the received signal, s is the transmitted signal, h is the channel impulse response, and w is the noise. The index $n = 4(i-1)+k$, $i = 1 : N$, refers to pressure (for $k = 1$), v_x, v_y, and v_z particle velocity components (for $k = 2, 3$, and 4, respectively), where N is the number of vector hydrophones. Thus, $n = 1$ is the pressure of the first VS, $n = 2$ is the v_x component, and so on. In (1), $\otimes$ stands for time convolution, and the noise is considered isotropic.

B. Methods and Measures

Figure 1 shows the proposed receiver based on the passive time-reversal. First, a noise normalization step aims to reduce the degradation of possible noisy channels. Readers can find a complete study regarding the impact of this normalization in [7]. A bank of correlators is used to estimate the time compression (Δ) between two subsequent preambles [8]. Then, Doppler compensation is performed using a resampling function (R), which is the input for the passive time-reversal.
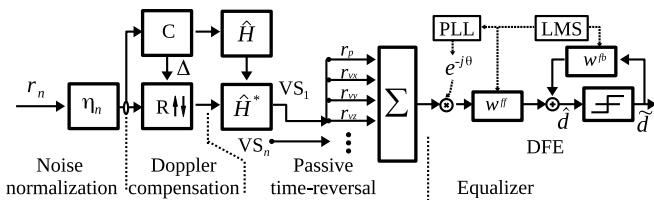
Fig. 1. VS passive time-reversal receiver. Input signals r_n are pressure and pressure-equivalent particle velocities. $\hat{H}$ is the estimated channel impulse response, and $[]^*$ stands for conjugate. Feed-forward and a feedback filter are $\mathbf{w}^{\mathrm{ff}}$ and $\mathbf{w}^{\mathrm{fb}}$. θ is a phase-carrier from PLL. $\hat{d}$ and $\tilde{d}$ are soft and hard decision symbols, respectively.

The time-reversal (active) is a method based on sound reciprocity, where a signal is transmitted by a single source (or a transducer array), received by an array of sensors (hydrophones or transducers), time-reversed, and retransmitted. In theory, the retransmitted signals will converge to the source position. This effect reminds a mirror, in which this method is also called time-reversal mirror [4], [9]–[11]. In the passive "version", the PTR performs a virtual play-back, convolving the received signals with the estimated channels for each receiver. Due to the low computational requirement, this method can be easily employed in real-time systems. However, in experimental data, channel variation can severely degrade its performance, and phase tracking algorithms followed by an equalizer are usually necessary [9].

The PTR output is given as [11]:

$$p(t) = \sum_{n=1}^{N} \hat{h}_n^*(-t) r_n(t). \tag{2}$$

Authors argue in favor of a single DFE to reduce computational requirements [5]. This study adopts a single DFE embedded by a second-order phase-locked loop (PLL) and implements a least mean square (LMS) algorithm. This option was adopted for simplicity since the objective is mainly in the vector hydrophone impact, not the equalizer itself. However, further analysis employing multichannel DFE may also benefit communications due to coherence issues, commonly reported in PTR studies [4], [11]. Ignoring the noise in (1) for convenience, ones obtain:

$$p(t) = \underbrace{\sum_{n=1}^{N} h_n(t)\hat{h}_n^*(-t)}_{q(t)} s(t), \tag{3}$$

where $q(t)$ is the sum of the channel's autocorrelation function, called PTR q-function. The q-function main-lobe to side lobes ratio shows the PTR capability to ISI mitigation. In fact, using a single channel ($N = 1$), the matched-filter output is obtained while increasing the number of sensors tends to reduce side-lobes effects (when diversity is explored).

Even though the q-function provides insights about the PTR focusing ability and ISI mitigation, it does not aim to quantify the channel's severity. In this regard, the rms delay-spread (DS) and spectral analysis are valuable measures. The former is given as [12]:

$$\sigma = \sqrt{\frac{\sum_k P(\tau_k)\tau_k^2}{\sum_k P(\tau_k)} - \left(\frac{\sum_k P(\tau_k)\tau_k}{\sum_k P(\tau_k)}\right)^2}, \tag{4}$$

where $P(\tau)$ is the power delay profile (see (4.4) of [13] for this estimation). The DS equation shown in (4) depends on the relative values of $P(\tau)$, in which a threshold is necessary. While the DS measure is convenient to quantify and compare multiple channels, the output to signal to noise ratio (OSNR) is generally adopted to quantify communication performance.

The OSNR provides a measure that includes the effect of the equalizer. The OSNR is given as [3]:

$$\text{OSNR}_{\text{dB}} = 10 \log \frac{N \sum_{n=1}^{N} \left[x(n) - \overline{x}(n) \right]^2}{\sum_{n=1}^{N} \left[x(n) - \tilde{d}(n) \right]^2}, \qquad (5)$$

where $x(n)$ is the transmitted symbol, $\overline{x}(n)$ is the time average of the transmitted symbol, and $\tilde{d}(n)$ is the hard-coded DFE output. The OSNR measure is interesting to provide, indirectly, the dispersion caused by ISI.

III. SIMULATION AND EXPERIMENTAL DATA RESULTS

Figure 2 shows the lateral view of a point-to-point communication system consisting of: a shallow-water area (100 m); four vector sensors forming a VSA with a spacing of 10 cm (30 cm total length); the VSA is vertically placed at 40 m depth; a bottom source at 90 m depth; source-VSA range is 907 m. This setup is used for simulation based on the Makai experiment (MakaiEx). Interested readers can find a complete description of this field experiment in [7], [14]. For simulation, the OASES numerical model provides the channel impulse response replicas for pressure, horizontal and vertical particle velocities [15]. The simulation uses the sound speed profile (SSP) measured during the MakaiEx and the bottom properties estimated in [16]. In the MakaiEx, each VS is composed of one pressure sensor and three uni-axial accelerometers.

The MakaiEx transmitted signal was a binary phase-shift keying (BPSK) in the carrier frequency of 10 kHz (2 kHz bandwidth). The message is a random sequence with 2 k symbol/s, where the first 127 is an m-sequence. The first 500 symbols of interleaved messages were used for Doppler compensation, channel estimation, and DFE training.

Figure 3 shows the estimated time-varying CIR for the y particle velocity component (horizontal). This CIR is Doppler compensated and normalized to the maximum value. The arrivals correspond to the direct path, bottom, surface, and bottom-surface reflections, respectively. One can notice that the third arrival presents a higher fading and amplitude (in several instants) than the direct path.
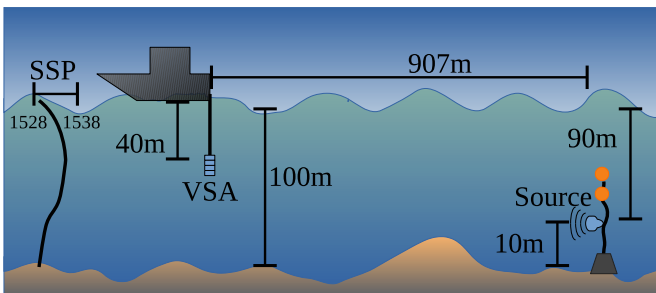
Fig. 2. Field experiment setup illustration. The VSA is tied at 40 m depth, a bottom-moored source is at 90 m (local place 100 m depth). Source-VSA range is 907 m. Sound speed varies from 1528 to 1538 m/s. These dimensions were used in simulation and are approximately the same as the verified in the MakaiEx.
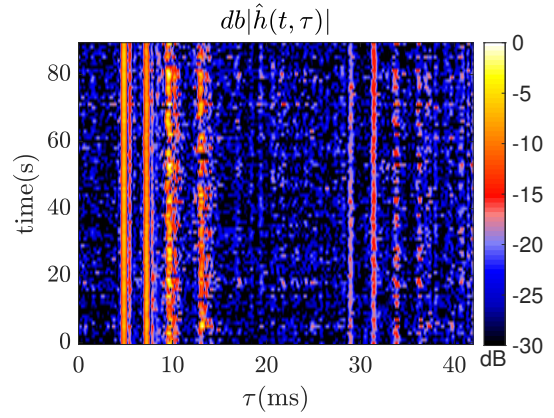
Fig. 3. Estimated channel impulse response (CIR) of y particle velocity component (VS#4). This time-varying channel was estimated using a preamble with 500 symbols for each 1 s message (90 s total).

Figure 4 shows the simulated CIR ("sim") and the estimated time-invariant CIR ("est") using the experimental data (normalized power delay profile, $P(\tau)$). Pressure (p) and particle velocity components (v_x, v_y, and v_z) are shown from top to bottom. Since the simulation only provides one horizontal component, we use $v_x = v_y$ for better visualization. The CIR from the experimental data was estimated using (4.4) of [13]. Moreover, in Fig. 4, a threshold of -15 dB is used for DS estimation.

Figure 5 shows the simulated CIR spectrum. The spectrum of the four pressure sensors is shown in Fig. 5 (a). Notice that a small spacing (10 cm) among sensors results in a diverse
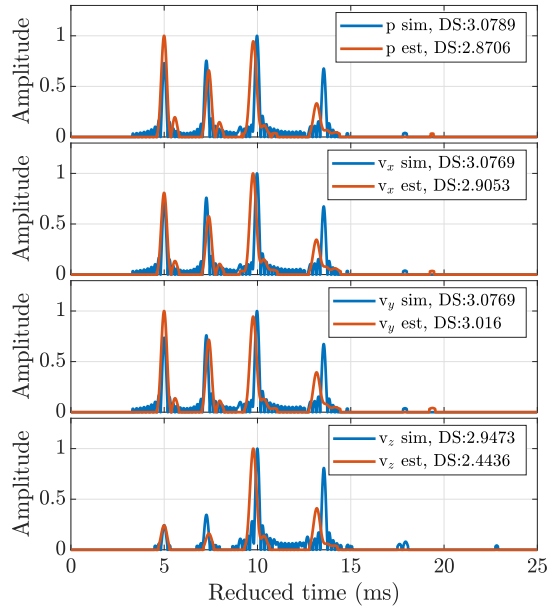
Fig. 4. Simulated and estimated power delay profile, $P(\tau)$, for pressure (p), and particle velocity components (v_x, v_y, v_z) from top to bottom, for VS#4. For simulation, OASES numerical model was used, and $v_x = v_y$, for visualization. The estimated $P(\tau)$ was obtained using (4.4) of [13] over the time-varying CIR. DS is shown for pressure and particle velocity components.
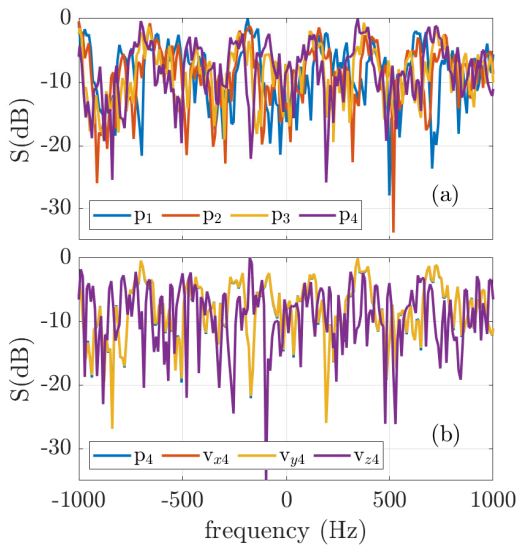
Fig. 5. Simulated CIR spectrum for pressure sensors (a), and pressure and particle velocity components of VS#4 (b).

spectral characteristic. The spectrum of VS#4 is shown in Fig. 5 (b), where one can notice that pressure and horizontal particle velocity ($v_x = v_y$) present high spectral similarity. On the other side, the vertical particle velocity presents distinct spectral characteristics compared to pressure and v_x.

CIR spectrum of the experimental data is shown in Fig. 6. Here, the spectral characteristics of the four pressure channels do not present a high level of diversity, as shown in the simulation (see Fig. 5 (a)). Moreover, nulls are present in several frequencies. For VS#4, the spectral characteristic is significantly diverse among VS channels.

The characteristics shown by CIR (power delay profile
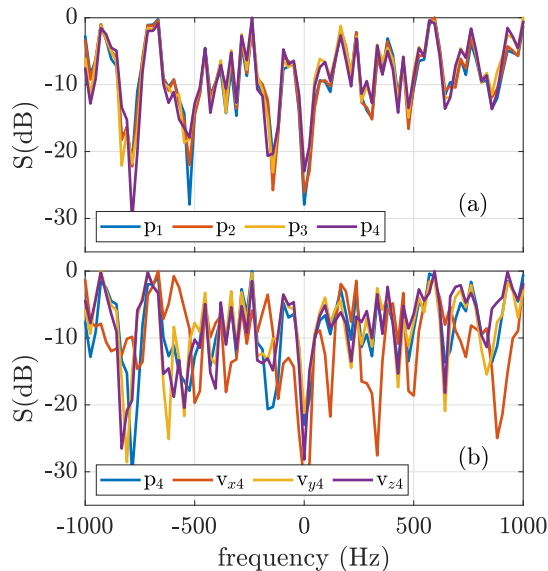
Fig. 6. Estimated CIR spectrum for pressure sensors (a), and pressure and particle velocity components of VS#4 (b).
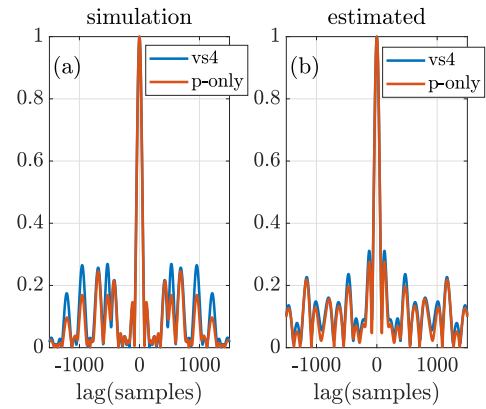
Fig. 7. PTR q-function for OASES simulation (a) and time-invariant estimated channel using experimental data (b).

and spectral) are interesting to understand the particularities of particle velocity channels compared to pressure channels. However, the effect of these channels in the communication signal processing chain is not directly noticed. In this regard, the q-function may provide useful information.

Figure 7 shows the PTR q-function for simulation (a), and experimental data (b). In both figures, the PTR q-function is calculated using (3), where "p-only" represent the q-function using four pressure sensors of the VSA, and "vs4" represents the q-function using the VS#4 channels (pressure and particle velocity components). Both figures show that using the pressure-only array or VS#4 result in similar side lobes.

The communication performance is shown in Table I for a single VS (VS#4), the pressure-only array (four hydrophones of the VSA), and the VSA. The performance is quantified by the OSNR and BER using OASES simulation, estimated time-invariant CIR (as shown in Fig. 4), and experimental data. The performance between VS#4 and p-only are similar in the three analyses, where the p-only performance is slightly better. For the estimated time-invariant CIR, a higher OSNR and lower BER are verified compared to the OASES simulation. Both previous results can be explained by: the DS showed in Fig. 4, where higher values are verified for OASES simulation; and the PTR q-function showed in Fig. 7, where side lobes are lower for the estimated channel than for OASES. The performance for VS#4 and p-only are degraded using the experimental data, where a coherence time of 500 ms is verified. The best performance is achieved using the VSA in the three analyses, in which superior performance is obtained.

TABLE I
COMMUNICATION PERFORMANCE FOR PRESSURE-ONLY ARRAY, A SINGLE VS AND VSA.

	OASES		Time-invariant CIR		Experimental	
	OSNR	BER	OSNR	BER	OSNR	BER
VS#4	8.45	3.34%	10.1	2.2%	3.16	6.43%
p-only	10.0	2.28%	10.6	1.95%	3.33	6.17%
VSA	16.44	0.33%	22.73	0.13%	4.15	2.55%

IV. Discussion

The PTR using pressure-only arrays is a method that explores channels' diversity. Authors have shown communication improvements provided by the PTR method, especially when arrays covering the water column are used. On the other hand, the performance is unavoidable reduced when small arrays are employed. In this regard, the spectral characteristic shown in Fig. 5 provides a first perception of how diversity can be achieved using a small pressure-only array or a single VS. Based on this simulation, we can infer that spectral nulls can be reduced (on average) even using the small pressure-only array, while for a single VS, the diversity is provided only by the vertical particle velocity.

The second phase of analysis consists of using the estimated channel from experimental data to quantify communication performance. This step is helpful since a time-invariant channel can be analyzed, considering an experimental component. Figure 6 shows that the pressure sensors present similar spectral characteristics, which is also an expected result since we are working with a 30 cm long array. The spectrum of VS#4 channels are diverse, which were not predicted by simulation. This result shows the challenge of characterizing such a sensor in a field experiment, where several factors may impact each channel differently.

The previous channels' analysis can indirectly explain the communication performance using simulation, time-invariant channel, and experimental data. However, the PTR q-function (Fig. 7) and the DS (Fig. 4) directly relate to the results. For instance, one can notice that DS values in the simulation are higher than using the estimated channel. In fact, the performance using the estimated channel is better than in simulation. Moreover, the PTR q-function shows that p-only provides slower side lobe amplitudes, which reflects on the results. Finally, based on the diversity found in VS#4 channels (see Fig. 6 (b)), it is expected that using multiples VS, this diversity increases. Thus, PTR using the VSA result in the best communication performance.

V. Conclusion

This paper investigates the PTR method using vector hydrophone channels to enhance underwater communications. While PTR is widely used with pressure-only arrays exploring diversity, it was not clear how vector hydrophones could provide diversity being a collocated device. We have seen that an ordinary PTR receiver structure used for pressure-only arrays can be directly used for vector hydrophones. This is a benefit of this method, where users can test the PTR method without vast knowledge about particle velocity channels, differently from steering methods [7]. However, the present work extends the usability of the PTR method, to question why using such channels is advantageous. In this regard, the study has shown by simulation and experimental data that diversity can be found among particle velocity channels. Spectral analysis shows that nulls (due to interference and fading effects) can be filled on average using VS channels. The performance comparison among a single VS, four-elements pressure-only array, and a VSA favors the use of vector hydrophones. Similar results were found for a single VS and pressure-only array, in which the performance of pressure-only comes with a larger size inconvenient. Moreover, the results entirely agree with the presented DS and q-function estimations. Finally, PTR may be an attractive method to explore VS channels due to its simplicity and low computational requirements, which is crucial for real-time applications used in autonomous platforms.

References

[1] M. Chitre, S. Shahabudeen, L. Freitag, and M. Stojanovic, "Recent advances in underwater acoustic communications networking," in *OCEANS*. Quebec City, QC: IEEE, Sep. 2008, pp. 1–10.

[2] M. Chitre, S. Shahabudeen, and M. Stojanovic, "Underwater acoustic communications and networking: Recent advances and future challenges," *J. Soc. Technol. Mar.*, vol. 42, no. 1, pp. 103–116, Mar. 2008.

[3] T. C. Yang, "A study of spatial processing gain in underwater acoustic communications," *IEEE J. Oceanic Eng.*, vol. 32, no. 3, pp. 689–709, Jul. 2007.

[4] J. Gomes, A. Silva, and S. Jesus, "Adaptive spatial combining for passive time-reversed communications," *J. Acoust. Soc. Am.*, vol. 124, no. 2, pp. 1038–1053, Aug. 2008.

[5] A. Song, A. Abdi, M. Badiey, and P. Hursky, "Experimental demonstration of underwater acoustic communication by vector sensors," *IEEE J. Oceanic Eng.*, vol. 36, no. 3, pp. 454–461, Jul. 2011.

[6] T. Gabrielson, "Design problems and limitations in vector sensors," Naval Undersea Warfare Center Division and Office of Naval Research, Newport, Rhode Island, Proceedings of the Workshop on Directional Acoustic Sensors, Apr. 2001.

[7] F. A. Bozzi and S. M. Jesus, "Acoustic vector sensor underwater communications in the Makai experiment," in *Proceedings of the 6th Underwater Acoustics Conference and Exhibition*. Virtual Meeting: Acoustical Society of America, Jul. 2021, p. 070029.

[8] B. Sharif, J. Neasham, O. Hinton, and A. Adams, "A computationally efficient doppler compensation system for underwater acoustic communications," *IEEE J. Oceanic Eng.*, vol. 25, no. 1, pp. 52–61, Jan. 2000.

[9] J. Flynn, J. Ritcey, D. Rouseff, and W. Fox, "Multichannel equalization by decision-directed passive phase conjugation: experimental results," *IEEE J. Oceanic Eng.*, vol. 29, no. 3, pp. 824–836, Jul. 2004.

[10] T. Yang, "Differences between passive-phase conjugation and decision-feedback equalizer for underwater acoustic communications," *IEEE J. Oceanic Eng.*, vol. 29, no. 2, pp. 472–487, Apr. 2004.

[11] J. Gomes, A. Silva, and S. Jesus, "Joint passive time reversal and multichannel equalization for underwater communications," in *OCEANS*. Boston, MA: IEEE, Sep. 2006, pp. 1–6.

[12] T. S. Rappaport, *Wireless communications: principles and practice*, 2nd ed. Upper Saddle River, N.J: Prentice Hall PTR, 2002.

[13] P. A. van Walree, "Channel sounding for acoustic communications: Techniques and shallow-water examples," Norwegian Defence Research Establishment (FFI), Tech. Rep. 2011/00007, Apr. 2011.

[14] M. Porter, B. Abraham, M. Badiey, M. Buckingham, T. Folegot, P. Hursky, S. Jesus, B. Kraft, V. McDonald, and W. Yang, "The makai experiment: high-frequency acoustics," in *Proceedings of the 8th European Conference on Underwater Acoustics*, Carvoeiro, Portugal, 12, p. 10.

[15] H. Schmidt, "Oases - user guide and reference manual," Department of Ocean Engineering Massachusetts Institute of Technology, Manual, Oct. 2004.

[16] P. Santos, O. C. Rodríguez, P. Felisberto, and S. M. Jesus, "Seabed geoacoustic characterization with a vector sensor array," *J. Acoust. Soc. Am.*, vol. 128, no. 5, pp. 2652–2663, Nov. 2010.